Multisite Mutagenesis of Interleukin 5 Differentiates Sites for Receptor Recognition and Receptor Activation†

Carmela G. Plugariu, Sheng-Jiun Wu, Wentao Zhang, and Irwin Chaiken*

Department of Medicine, University of Pennsylvania School of Medicine, 909 Stellar Chance Laboratories, 422 Curie Boulevard, Philadelphia, Pennsylvania 19104

Received June 27, 2000; Revised Manuscript Received September 18, 2000

ABSTRACT: Multisite mutagenesis of single-chain and monomeric forms of human interleukin 5 (IL-5) was performed to investigate mechanistic features of receptor activation and the possibility of differentiating sites of activation from those for receptor interaction. The normally dimeric human IL-5 contains two domains, each containing a four-helix bundle. IL-5 has previously been re-engineered into the monomeric, one-domain GM1 form by introducing an eight-residue linker between the third and fourth helices. In this study, we tested a combination of mutations in a single-chain IL-5 (scIL-5) construct, [^{89}SLRGG^{92},W^{110}/^{89}AAAAA^{92},A^{110}]scIL-5. This mutein was found to retain substantial IL-5 receptor α-chain binding but with selectively suppressed proliferation of the IL-5-dependent cell line TF-1.28. This result confirms recent findings that IL-5 receptor α-chain recognition can be supported by the ^{89}SLRGG^{92} epitope and that, in contrast, Glu110 is important in receptor activation. On the basis of this result, two mutants of GM1 were constructed with the intent to retain receptor α-chain binding while modifying receptor activation epitopes. In the first, [^{88}SLRGG^{92},W^{110}]GM1, the wild-type CD-loop sequence ^{89}EERRR^{92} was converted to the mimotope ^{89}SLRGG^{92}, and Glu110 to Trp. In the second, [A^{13},A^{110}]GM1, wild-type Glu13, and Glu110 were both mutated to Ala. GM1 and mutants were expressed in high yield in *Escherichia coli*, purified under denaturing conditions from inclusion bodies, and refolded. Monomers were screened for binding to shIL-5Rα-Fc using optical biosensor and ELISA and for bioactivity by proliferation of TF-1.28 cells. Both [^{88}SLRGG^{92},W^{110}]GM1 and [A^{13},A^{110}]GM1 were found to interact with the shIL-5Rα-Fc, with affinities of 69−585 nM, 2−15-fold weaker than that of the original GM1. The mutants also were able to compete with IL-5 for binding to shIL-5Rα in an ELISA. In contrast, both mutants exhibited a disproportionately decreased capacity to stimulate TF-1.28 cell proliferation. [A^{13},A^{110}]GM1 bioactivity was 160-fold lower than that of GM1, while that for the [^{88}SLRGG^{92},W^{110}]GM1 mutant was 2600-fold lower. The largely retained IL-5 receptor α-chain binding affinities versus relatively suppressed bioactivities of [A^{13},A^{110}]GM1 and [^{88}SLRGG^{92},W^{110}]GM1 variants, in particular the latter, point to the existence of separable IL-5 epitopes for receptor binding and activation and establish the potential to design smaller IL-5 mimetic antagonists.

Interleukin-5 (IL-5)[1] is the key cytokine involved in the maturation, proliferation, and activation of eosinophils, which have been implicated in the pathogenesis of asthma and other allergic inflammatory diseases associated with hypersensitivity reactions in the lung (*1*−*3*). The association of eosinophilia with these chronic inflammatory conditions has suggested that blocking the action of IL-5 might provide therapeutic benefit for the allergic disorders.

IL-5 exerts its biological functions through binding to a heteromeric cell surface receptor. The IL-5 receptor is composed of two subunits, α and β_c, that belong to the superfamily of cytokine receptors typified by the growth hormone receptor (*4*−*6*). The α-chain is IL-5-specific, though structurally related to the α-chains for GM-CSF and IL-3 receptors. The β_c-chain is identical to the β-chains of GM-CSF and IL-3 receptors (*7*, *8*), hence the denotation β_c for common β. The extracellular domain of the α-subunit can bind to IL-5 in the absence of the β_c-chain (*7*, *9*, *10*). The human α-chain alone binds IL-5 with a K_d of 0.3−0.6 nM when expressed in *COS7* cells (*9*). The β_c-subunit is essential for signaling. The β_c-subunit also contributes to ligand binding (*10*, *11*), as indicated by several findings, including the increased (2−4-fold) hIL-5 binding affinity when α- and β_c-chains are coexpressed (*12*). However, direct binding of IL-5 to the β_c-chain alone has never been quantitated.

† This work was supported by NIH R01 Grants GM55648 (I.C.) and AI40462 (I.C.) and American Cancer Society Grants RPG-95-072-04 (I.C.).

* To whom correspondence should be addressed: Rheumatology Division, Department of Medicine, 909 Stellar Chance Laboratories, University of Pennsylvania School of Medicine, 422 Curie Blvd., Philadelphia, PA 19104. E-mail: chaiken@mail.med.upenn.edu. Phone: (215) 573-9678. Fax: (215) 349-5572.

[1] Abbreviations: IL, interleukin; hIL, human interleukin; scIL, single-chain human interleukin; EDC/NHS, 1-ethyl-3-[3-(dimethylamino)-propyl]carbodiimide hydrochloride/*N*-hydroxysuccinimide; shIL-5Rα, soluble human interleukin-5 receptor α-chain; shIL-5Rα-Fc, soluble human interleukin-5 receptor α-chain−Fc chimera; GM-CSF, granulocyte macrophage colony-stimulating factor; PCR, polymerase chain reaction; ELISA, enzyme-linked immunosorbent assay; mAb, monoclonal antibody; PBS, phosphate-buffered saline; MTT, 3-(4,5-dimethylthiazol-2-yl)-2,5-diphenyltetrazolium bromide (thiazolyl blue).

10.1021/bi001467p CCC: $19.00
Published on Web 11/10/2000

Glycosylation of IL-5 is not required for activity, as the human recombinant protein produced in *Escherichia coli* is fully active (*13*). The crystal structure of *E. coli*-derived IL-5 shows that the disulfide-linked dimer forms two domains each containing four helices packed with the cytokine fold (*14*). The cytokine fold is common among other members of the four-helix bundle cytokine family which includes GM-CSF and growth hormone (*4*). However, the other four-helix bundle cytokines are monomeric. Monomeric IL-5 has been engineered by extension of the loop linking the third and fourth helices (*15*−*18*). This allows the protein to fold in a manner similar to that of GM-CSF. Monomeric IL-5 has been found to be substantially active, though somewhat less so than the dimer. The residues of IL-5 required for receptor interaction have been mapped by extensive mutagenesis studies (*19*−*22*). Residues important for IL-5 receptor α-chain binding have been identified in the C-terminal region, including Glu110 on the fourth (D) helix and Glu89 and Arg91 on the *β*-sheet preceding the D helix. Recent epitope randomization analysis using phage-displayed scIL-5 has shown that the sequence ^{89}EERRR^{92} can be replaced with SLRGG with retention of IL-5 receptor α-chain binding, suggesting that the importance of Glu89 and Arg91 residues involves their role in promoting a charge balance in the sequence of residues 88−92 (*23*). Glu13 on the first (A) helix has been shown to be important for receptor activation but not IL-5 receptor α-chain binding (*19*, *24*). Since IL-5 monomers are substantially active, it appears that only one set of residues (Glu89, Arg91, Glu110, and Glu13) is needed for receptor binding and activation.

Epitope randomization mutagenesis of single-chain IL-5 molecules has also been used to identify a role for Glu110 in receptor activation (*25*). Examination of mutants with all possible naturally occurring amino acid residues at position 110 showed that residue replacements which enabled retention of IL-5 receptor α-chain binding included Trp and Tyr (*25*). Strikingly, however, Trp replacement disproportionately reduced bioactivity, except when Glu110 was present in the neighboring four-helix bundle domain. This result suggested that the negative charge at Glu110 was important for receptor activation, though dispensable for α-chain binding.

The results from epitope randomization studies, in particular the realization that Glu110 played a role in receptor activation, led us to design combination mutations, in scIL-5 and monomeric IL-5, which could help yield a further understanding of receptor activation and which might provide protein antagonist leads more effective than those made previously. For a monomeric IL-5 structural background, we used both scIL-5 and GM1, both of which could be expressed in high yield in *E. coli*. GM1 was previously shown to be significantly active and stable (*15*). The combined mutations we made, in both single-chain IL-5 and GM1 backgrounds and containing Glu110 replacements in combination with other mutations, resulted in IL-5 muteins that are stronger partial antagonists than those obtained previously with the Glu13 mutation alone. The results emphasize the separability of binding and activation epitopes in IL-5 and support the notion that it may be feasible to design smaller molecule mimetic antagonists of IL-5 by retaining receptor binding epitopes but eliminating those for receptor activation.

EXPERIMENTAL PROCEDURES

Reagents. Unless otherwise stated, all chemicals were purchased from FisherBiotech. Enzymes were from Boehringer Mannheim, and oligonucleotides were purchased from the Genetics Core Facilities of the University of Pennsylvania.

Construction of the Single-Chain IL-5 Mutant, [^{88}SLRGG^{92}, W^{110}/^{88}AAAAA^{92},A^{110}]scIL-5, by Site-Directed Mutagenesis. The phagemid vector, pMK-wt/A5-G3 (*23*, *25*), was used as a starting point to prepare a single-chain IL-5 mutant as a protein antagonist lead. The Glu110 residues were mutated to either a Trp or Ala, and the CD loop (^{88}EERRR^{92}) was mutated to either ^{88}SLRGG^{92} or ^{88}AAAAA^{92} using a QuickChange site-directed mutagenesis kit (Stratagene). The combination of mutations in the N-terminal and C-terminal halves of scIL-5 yielded an asymmetric mutant phagemid, designated as pMK-[^{88}SLRGG^{92},W^{110}/^{88}AAAAA^{92},A^{110}]scIL-5. The resulting construct was verified by DNA sequencing.

E. *coli Expression and Purification of [^{88}SLRGG^{92},W^{110}/^{88}AAAAA^{92},A^{110}]scIL-5.* The phagemid vector pHage 3, which is derived from M13, was used for protein expression (Maxim Biotech). The scIL-5 mutant gene was amplified using PCR, with primers that introduced *Sal*I and *Apa*I restriction sites. The resulting PCR fragment was digested with *Sal*I and *Apa*I and ligated into the *Sal*I−*Apa*I sites of pHage 3 phage vector, yielding pH3-[^{88}SLRGG^{92},W^{110}/^{89}-AAAAA^{92},A^{110}]scIL-5.

The mutant plasmid was transformed into *TOPP3* cells (Stratagene). The recombinant cells were grown in super broth medium and induced with 1 mM IPTG as described previously (*23*). The lysate supernatant from the induced culture was dialyzed against PBS buffer (pH 7.4) and then loaded onto two monoclonal anti-IL-5 affinity columns (in series) equilibrated in PBS buffer. The two affinity columns were packed with mAb 2E3-Sepharose 4B matrix and mAb 4A6-Sepharose 4B matrix. The 2E3 mAb is a neutralizing antibody that blocks IL-5 interaction with the α-chain of the IL-5 receptor complex (*23*, *26*). Conversely, 4A6 mAb is an activity-neutralizing antibody whose exact binding epitope is presently unknown but which does not block IL-5 interaction with the receptor α-chain (*23*). The protein was eluted with 0.1 M glycine (pH 2.5). The final yield of the [^{88}SLRGG^{92},W^{110}/^{88}AAAAA^{92},A^{110}]scIL-5 mutant was analyzed by SDS−10% polyacrylamide gel electrophoresis (SDS−PAGE) according to the method of Laemmli (*27*).

Construction of the pET19b-GM1 Expression Vector for the IL-5 Monomer and Muteins. The IL-5 monomer GM1 gene (*15*) was amplified by PCR using the forward primer 5′-ACGACCATATGGCCAGATCTGAAATTCCC-3′ and the reverse primer 5′-GAGAGGATCCTTATCAACTTTC-TATTATCC-3′ with *Nde*I and *Bam*HI restriction sites introduced (underlined). The resulting PCR product (∼350 bp) was digested with restriction endonucleases *Nde*I and *Bam*HI, purified on a 1% agarose gel, and finally ligated into the pET19b vector (Novagen). The ligated vector was transformed into the *E. coli* BL21(DE3) Codon Plus strain (Stratagene). The resulting mutants were verified by DNA sequencing.

Multisite Mutagenesis of GM1. The mutation of ^{88}EE-RRR^{92} to ^{88}SLRGG^{92} or ^{88}AAAAA^{92} in the CD loop and Glu13 or Glu110 to Ala and Trp, respectively, was performed using a QuickChange site-directed mutagenesis kit (Stratagene). The combined mutations of both Glu110 and Glu13

to Ala led to a mutant that was designated [A^{13},A^{110}]GM1. The mutant containing ^{88}SLRGG^{92} in the CD loop and Trp110 instead of Glu110 was designated [^{88}SLRGG^{92},W^{110}]-GM1.

Expression of GM1 and GM1 Mutants in E. coli. Flasks (2 L) each containing 1 L of LB medium (100 μg/mL ampicillin) were inoculated with 10 mL from an overnight culture of *E. coli* BL21(DE3) Codon Plus (Stratagene), transformed with the pET19b-GM1 or pET19b-GM1 mutant. The flasks were shaken in an air shaker at 37 °C until an OD_{600} of 0.6 was attained. Then, IPTG was added to a final concentration of 0.4 mM to induce protein expression. The cells were harvested 3 h postinduction by centrifugation at 4 °C (6000*g* for 10 min) in a Sorval centrifuge.

Protein Purification and Refolding. All steps were carried out at 4 °C, except where stated. GM1 mutants were monitored by SDS−PAGE. The proteins of interest were found to accumulate during expression in the form of inclusion bodies. Hence, the protein was initially solubilized under denaturing conditions and purified under these denaturing conditions, using a Ni−NTA affinity support (Qiagen). Refolding was carried out in the presence of 2 M urea following a protocol outlined previously (*13*).

E. coli BL21 cells were suspended in 0.1 M phosphate buffer (pH 8.0) and lysed by sonication. The suspension was then centrifuged at 10000*g* for 30 min. The pellet was suspended in a denaturing buffer composed of 0.1 M Tris-HCl (pH 8.5), 6 M guanidinium chloride (Gibco BRL), and 10 mM imidazole (Sigma) and stirred for 1 h. The suspension was centrifuged again at 10000*g* for 30 min, and 1 mL of the Ni−NTA matrix was added to each 100 mL of clear supernatant. After being stirred for 1 h, the resin−protein complex was packed into a column and washed with 10 times the column volume of a washing buffer consisting of 0.1 M Tris-HCl (pH 8.5), 6 M guanidinium chloride, and 20 mM imidazole. The protein was eluted with 0.1 M Tris-HCl (pH 8.5), 6 M guanidinium chloride, and 250 mM imidazole. The fractions containing the protein were pooled together and dialyzed overnight against 0.1 M Tris-HCl (pH 8.5), 6 M urea (Gibco BRL), and 1 mM DTT. The solution was then diluted with an appropriate volume of buffer containing 0.1 M Tris-HCl (pH 8.5) and urea so that the final urea concentration was 2 M and the protein concentration did not exceed 50 μg/mL. The solution was stirred for 24 h and then dialyzed against 40−50 times the volume of 0.1 M Tris-HCl (pH 8.5). The dialysis was carried out over a period of 24 h, with two buffer changes. The protein was refolded at this stage. Any insoluble protein was removed by filtration through a 0.22 μm cellulose acetate membrane filter (Corning). For further experiments, the protein was dialyzed against PBS buffer (pH 7.4) and concentrated by ultrafiltration on an Amicon YM3 filter to a concentration up to 1 mg/ml. The concentrations of purified proteins were estimated as described by Bradford. For a more definitive determination, the concentrations of the mutant proteins were measured with Western blot analysis and with the quantitative IL-5 enzyme-linked immunosorbent assay (ELISA) using the monoclonal antibodies 4A6 and TRFK-5 (R&D Systems).

Analysis of the Apparent Molecular Mass and Aggregation State. The sizes of expressed scIL-5 and GM1 proteins were evaluated using a Bio-Rad FPLC system, with a Superose 12 HR 10/30 (Pharmacia Biotech) size exclusion analytical column equilibrated with 20 mM sodium phosphate (pH 7.4) containing 150 mM NaCl. The column was calibrated with standards with known molecular masses (Bio-Rad), and 240 μL of each mutant was applied at concentrations between 400 and 700 μg/mL.

Circular Dichroism Measurements. Spectra were recorded on an Aviv 62A DS CD spectropolarimeter. Proteins were scanned repetitively in 0.1 cm quartz cuvettes from 190 to 280 nm in 1 nm wavelength increments. Ellipticity was converted to molar residual ellipticity for comparisons. Solution conditions included 10−20 μM protein (pH 7.4), 20 mM sodium phosphate, and 150 mM NaCl at 25 °C. Thermal stabilities of protein constructs were evaluated by monitoring the ellipticity at 222 nm. The temperature was increased in each case at a rate of 30 °C/h.

Biological Activity. The mutants were assayed for activity using a highly responsive subclone of the human erythroleukemia cell line TF-1.28 and MTT [3-(4,5-dimethylthiazol-2-yl)-2,5-diphenyltetrazolium bromide (thiazolyl blue)] (Sigma) (*28*). Cells were cultured in RPMI 1640 medium supplemented with L-glutamine, penicillin/streptomycin, and 10% heat-treated fetal calf serum (Life Techniques, Inc.). Plates with 96 flat-bottomed wells were seeded with 5000 cells/well and incubated for 48 h in triplicate in the presence of serially diluted single-chain IL-5 or mutant proteins. Then, 10 μL of 5 mg/mL MTT in 1× PBS was added per well, and after 5 h, 100 μL of 10% SDS in 0.01 N HCl was added to solubilize the precipitated crystals. After overnight incubation at 37 °C, absorbance at 570 nm was measured. EC_{50} values were determined by fitting to a four-parameter equation to determine the concentration of the mutants that resulted in half-maximal TF-1 cell proliferation.

*Competitive ELISA for Assessing Binding of scIL-5 and GM1 Mutants to shIL-5R*α. Competitive ELISAs on microtiter plates coated with single-chain IL-5 were performed to confirm the relative receptor binding affinities of different mutants according to a protocol outlined previously (*29*). PRO-BIND ELISA plates (Falcon) were coated with 100 μL (20 μg/mL) of single-chain IL-5 (*30*) in PBS buffer (pH 7.4). Protein-charged ELISA plates were incubated overnight at 4 °C with 100 μL of 50 nM shIL-5Rα (*31*) and different concentrations of singl- chain IL-5 or GM1 mutants ranging from 0 to 40 μM in PBS buffer. The wells then were washed five times with PBS and 0.5% Tween 20 (PBST). shIL-5Rα bound to scIL-5 was detected with a 1:1000 dilution of anti-human IL-5Rα (PharMingen), followed by a 1:3000 dilution of horseradish peroxidase-conjugated rabbit mouse IgG (DAKO A/S) and color development with 3,3′,5,5′-tetramethylbenzidine dihydrochloride (Sigma). This reagent was dissolved in 0.05 M phosphate/citrate buffer (pH 5.0) containing 0.03% sodium perborate (Sigma). The reaction was assessed by the absorbance at 450 nm. Mouse IgG that bound to the microtiter plate was used as a background control.

Kinetic Analysis of Receptor Binding by scIL-5 and GM1 Mutants. Kinetic and equilibrium constants for the interaction between the IL-5 receptor α-chain and *E. coli*-expressed single-chain IL-5 or GM1 mutants were measured using a BIA 3000 optical biosensor (Biacore Inc., Uppsala, Sweden). Experiments were performed at 25 °C in PBS buffer (pH 7.4) with 0.005% Tween 20. Immobilization of the ligand or the antibody (IL-5Rα-Fc or 4A6) to either CM5 or B1 sensor chips was performed following the standard amine coupling procedure according to the manufacturer's speci-

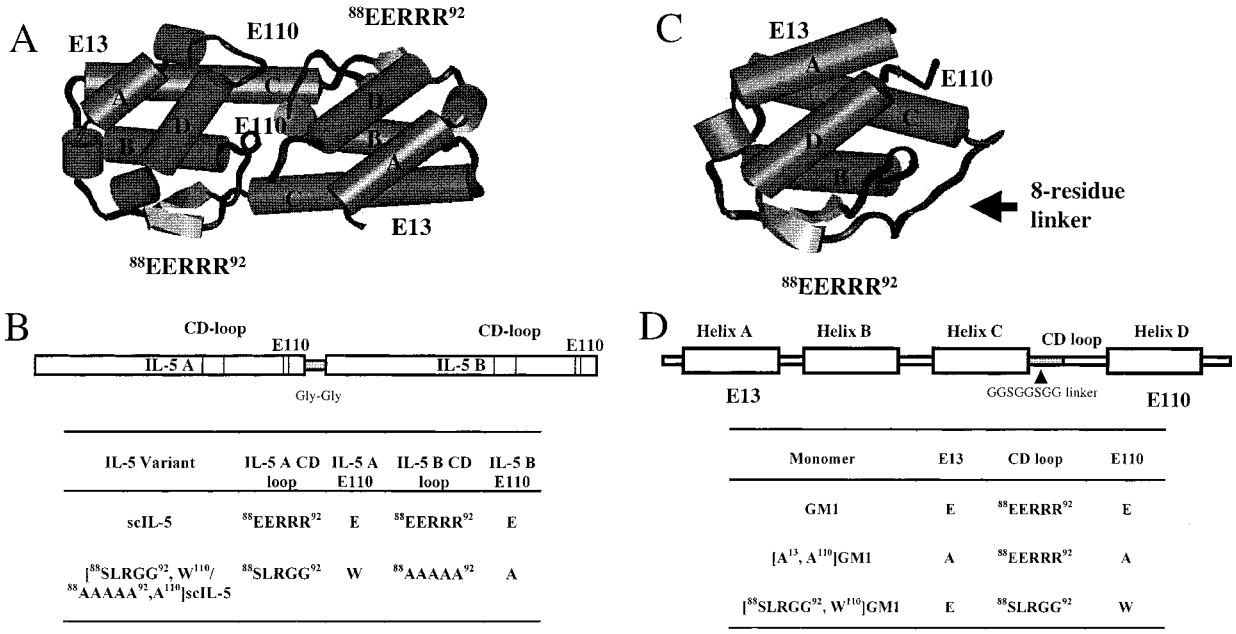

IL-5 Variant	IL-5 A CD loop	IL-5 A E110	IL-5 B CD loop	IL-5 B E110
scIL-5	^{88}EERRR^{92}	E	^{88}EERRR^{92}	E
[^{88}SLRGG^{92}, W^{110}/ ^{88}AAAAA^{92},A^{110}]scIL-5	^{88}SLRGG^{92}	W	^{88}AAAAA^{92}	A

Monomer	E13	CD loop	E110
GM1	E	^{88}EERRR^{92}	E
[A^{13}, A^{110}]GM1	A	^{88}EERRR^{92}	A
[^{88}SLRGG^{92}, W^{110}]GM1	E	^{88}SLRGG^{92}	W

FIGURE 1: Molecular models of single-chain IL-5 and monomeric GM1 and a schematic representation of the designed IL-5 constructs. (A) Single chain IL-5 model. (C) GM1 model. The location of the IL-5 receptor binding epitopes Glu13 on helix A, Glu110 at the C-terminus, and the CD loop sequence comprising residues 88−92 between helices C and D are indicated in the single-chain IL-5 and GM1 models. The figures were generated using INSIGHT version 98.0 (Molecular Simulations, Inc.). (B) The gene of the single-chain IL-5 was constructed by linking two hIL-5 genes in tandem separated by a spacer that encoded the G-G dipeptide. The amino-terminal half of the molecule is defined as IL-5A and the carboxyl-terminal half as IL-5B. An asymmetric scIL-5 mutant, denoted [^{88}SLRGG^{92},W^{110}/^{88}AAAAA^{92},A^{110}]-scIL-5, was composed of an N-terminal half containing the five original charged residues (^{88}EERRR^{92}) in the CD loop combined with a C-terminal half containing a functionally disabling CD loop sequence (^{88}AAAAA^{92}) and the Glu110 replaced with Ala. (D) Schematic representation of the monomeric mutants. Helices A−D are shown as open boxes. The GGSGGSGG linker is shown as a shaded box.

fication. Briefly, carboxyl groups on the sensor chip surface were activated by injection of 35 μL of a solution containing 0.2 M EDC and 0.05 M NHS at a flow rate of 5 μL/min. Then, a protein ligand at a concentration of 15 μg/mL in 10 mM NaOAc buffer (pH 5.0) was passed over the chip surface at a flow rate of 5 μL/min. One or more reference surfaces that were used as a background to correct for instrument and buffer artifacts were generated at the same time under the same conditions with omission of the protein ligand. BSA was used as a negative control.

In a "sandwich assay", the monoclonal antibody 4A6 was first immobilized onto the biosensor chip (*15*) and the purified single-chain IL-5 or GM1 mutant was anchored noncovalently to the antibody. The binding of shIL-5Rα-Fc at various concentrations (*31*) to the antibody-anchored single-chain IL-5 or GM1 mutant protein was then assessed. Alternatively, in a "direct assay", shIL-5Rα-Fc was directly immobilized on the sensor chips, and single-chain IL-5 or GM1 variants were used as analytes.

The rate constants for binding of single-chain IL-5 or GM1 to the receptor were calculated by globally fitting the association and dissociation phases of sensorgrams obtained either for a series of soluble shIL-5Rα-Fc concentrations in the sandwich assay or for a series of single-chain IL-5 or GM1 mutant concentrations in the direct binding assay. Fits were to a 1:1 Langmuir model (A + B ⇔ AB). These fits automatically incorporated bulk phase refractive index adjustments where appropriate. This type of analysis yielded, for each single-chain IL-5 and GM1 mutant, an association rate constant k_a, a dissociation rate constant k_d, and an equilibrium dissociation constant, K_d, as the ratio k_d/k_a. Biosensor results are reported as a mean of three determinations. Data analysis was conducted using the BIAcore evaluation software (version 3.0).

Molecular Modeling. Single-chain IL-5 and GM1 molecules were modeled using the X-ray crystal structure of IL-5 (*14*) obtained from the Protein Data Bank (PDB entry 1hul). Modeling was performed using the software package INSIGHT version 98.0 (Molecular Simulations, Inc., San Diego, CA) on a Silicon Graphics O2 workstation. The scIL-5 was designed by introducing a Gly-Gly linker that connected the C-terminal Ile112 of IL-5 unit A with the N-terminal Ile5 of IL-5 unit B. The residues in the CD loop and 110 positions were replaced via the designed mutations. A GM1 model was obtained by inserting an eight-residue (Gly-Gly-Ser-Gly-Gly-Ser-Gly-Gly) linker just after Lys85 from the first unit, following Cys86 of the second unit of the IL-5 structure. The resulting structures were subjected to 1000 steps of conjugate gradient energy minimization. The derivative was set to 0.05 kcal/mol, and the output files were monitored for gradient convergence.

RESULTS

Protein Design. To evaluate the separability of receptor binding and activation epitopes in the intrinsically dimeric IL-5 molecule, two protein redesign strategies were used in this work. The first was to design a single-chain IL-5 molecule containing a functional N-terminal domain and a mutationally disabled C-terminal domain. The N-terminal half contained a simplified CD loop, the mimotope SLRGG (*23*), combined with the mutation of Glu110 to Trp (*25*, *30*, *32*). The functional disabling of the C-terminal half was achieved by replacing ^{88}EERRR^{92} and Glu110 with six Ala residues (see Figure 1A,B). The resulting construct was designated [^{88}SLRGG^{92},W^{110}/^{88}AAAAA^{92},A^{110}]scIL-5.

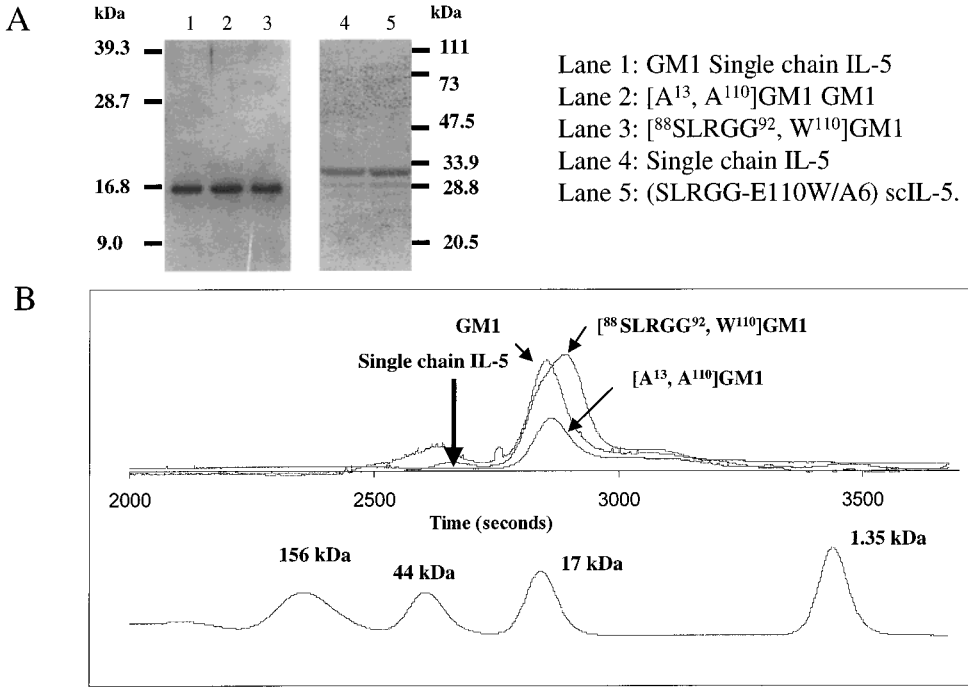

FIGURE 2: SDS−polyacrylamide gel electrophoresis and gel filtration analysis of *E. coli*-expressed single-chain IL-5 and GM1 mutants. (A) SDS−PAGE scans of gels with Coomasie staining. (B) Size exclusion chromatography using an analytical scale Superose 12 column: upper panel, overlaid chromatograms of GM1, [A^{13},A^{110}]GM1, and [^{88}SLRGG^{92},W^{110}]GM1 as indicated by arrows; lower panel, chromatogram of Bio-Rad standards with known molecular masses. GM1 constructs have a calculated molecular mass of 16.8 kDa, and they elute at about the elution time corresponding to the 17 kDa equine myoglobin marker. The single-chain IL-5, with a molecular mass of 30 kDa, was eluted as indicated with the arrow.

The second protein redesign strategy utilized the ability to form functional IL-5 monomers. Increasing the length of the loop between helices C and D so the loop resembles the loop of GM-CSF has been found previously to allow IL-5 helix D to fold within its parent monomer (*15*−*17*). The construct in which a GGSGGSGG linker was inserted after Lys85 in the original sequence of IL-5 (*15*) was previously designated GM1 (Figure 1C,D). The forms of GM1 made in this study are shown in Figure 1D and are defined as follows. [A^{13},A^{110}]GM1 had residues Glu13 and Glu110 mutated to Ala. The CD loop and Glu110 combined mutant, in which ^{88}EERRR^{92} was replaced with the mimotope SLRGG and Glu110 was mutated to a Trp, was designated [^{88}SLRGG^{92},W^{110}]GM1.

Protein Characterization. To study the potential functional properties of the designed single-chain IL-5 and GM1 mutants, the proteins were expressed and purified from *E. coli*. By SDS−PAGE, the soluble scIL-5 mutant expressed in *E. coli* was detected as a single band of approximately 30 kDa in the supernatant after IPTG induction, as expected for recombinant proteins that are secreted into the periplasm. The purified [^{88}SLRGG^{92},$W^{110/89}$AAAAA^{92},A^{110}]scIL-5 also behaved as a single band of approximately 30 kDa (Figure 2A).

The monomeric constructs were expressed in high yield with a 10-His N-terminal tag (see Experimental Procedures). They were purified from inclusion bodies, providing yields of 1 mg of purified protein from 1 L of bacterial culture. The purity of the refolded proteins was checked by SDS−PAGE, revealing a single band of approximately 16.8 kDa (Figure 2A), the molecular mass of the GM1-His tag construct. Similar masses were detected on nonreducing SDS−PAGE, demonstrating that there was no formation of intermolecular disulfide bonds (results not shown).

The aggregation state of the GM1 constructs was further assessed by size exclusion chromatography. When subjected to gel filtration at concentrations between 400 and 700 μg/mL, the GM1 proteins eluted close to the volume observed for the equine myoglobin marker (molecular mass of 17 kDa) (Figure 2B). This indicated that they were in a monomeric state and did not self-associate as dimers or oligomers in the buffer conditions used for binding experiments, TF-1 cell proliferation, and circular dichroism.

Correct folding of the purified proteins was established by circular dichroism spectroscopy. CD spectra (190−260 nm) of all the single-chain IL-5 and monomeric constructs were consistent with high α-helical content (Figure 3). The various mutations introduced in this work did not appear to perturb the overall secondary structure elements, as shown by the overlap of mutant and parent spectra for both the scIL-5 and GM1 cases. The monomers were found to be less stable than the parent wild-type IL-5 ($T_{1/2}$ = 71.1 °C) (*16*), as judged from the temperature dependence curves shown in panels B and D of Figure 3. Importantly though, all of the mutants were predominantly folded into helix-rich conformations at the temperatures used for subsequent receptor binding and bioactivity assays, namely, 25 and 37 °C, respectively.

Binding and Bioactivity Properties of [^{88}SLRGG^{92},W^{110}/^{88}AAAAA^{92},A^{110}]scIL-5. The ability of the asymmetrically disabled single-chain IL-5 mutant designated [^{88}SLRGG^{92},W^{110}/^{88}AAAAA^{92},A^{110}]scIL-5 (Figure 1A,B) to bind the receptor α-chain was tested using an optical biosensor via protocols similar to those described previously (*22*, *23*, *25*, *31*), in

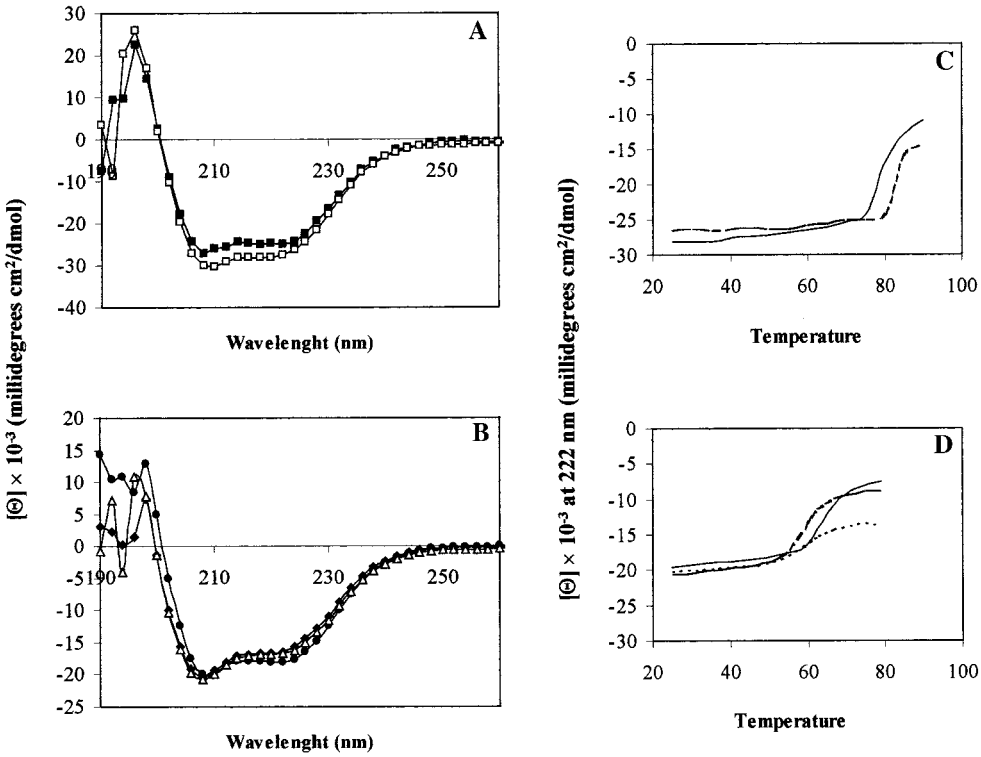

FIGURE 3: Circular dichroism spectra of IL-5 constructs. The spectra are given as molar residual ellipticity (millidegrees per square centimeter per decamole) vs wavelength. Overlays of averaged spectra from three scans each of (A) single-chain IL-5 (■) and [^{88}SLRGG^{92},W^{110}/^{88}AAAAA^{92},A^{110}]scIL-5 (□) and (B) GM1 (◆), [A^{13},A^{110}]GM1 (△), and [^{88}SLRGG^{92},W^{110}]GM1 (●) are shown. The thermal stabilities of (C) the single-chain IL-5 (solid line) and [^{88}SLRGG^{92},W^{110}/^{88}AAAAA^{92},A^{110}]scIL-5 (dashed line) and (D) GM1 (solid line), [A^{13},A^{110}]-GM1 (dashed line), and [^{88}SLRGG^{92},W^{110}]GM1 (dotted line) also are shown. Thermal stabilities were evaluated by monitoring the ellipticity at 222 nm in a temperature range from 25 to 90 °C.

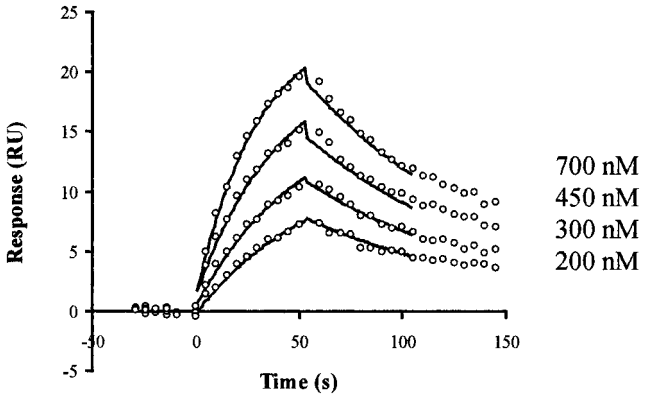

FIGURE 4: Sensorgram overlays for [^{88}SLRGG^{92},W^{110}/^{88}AAAAA^{92}, A^{110}]scIL-5 binding to shIL-5Rα-Fc at different analyte concentrations. The analyte concentrations are shown at the right of each sensorgram. Immobilization of shIL-5Rα-Fc was carried out directly on the sensor chip, at a surface density of 2000 RU. The rate constants for binding to shIL-5Rα-Fc were calculated by globally fitting the association and dissociation phases of the sensorgrams to a 1:1 Langmuir model (A + B ⇔ AB), as described in Experimental Procedures.

particular, a direct binding assay protocol. The shIL-5Rα-Fc was immobilized on the sensor chip, and scIL-5 was used as the analyte. A surface density of 2000 RU was generated by direct immobilization through amine coupling. Use of this surface at different flow rates allowed us to eliminate mass transport as a limiting factor in observed binding kinetics and to optimize experimental conditions. Sensorgrams for this analysis are shown in Figure 4. Kinetic association and dissociation rate constants were obtained by global fitting of the biosensor data to a simple 1:1 binding model. To test for the possible contribution of mass transport, we fit the sensor data to a mass transport model (*33*). However, the latter showed no improvement in χ^2, and the K_m (mass transport contribution) was insignificant compared to k_{on}. The resulting data fits are shown in Figure 4, and the kinetic and equilibrium constants are summarized in Table 1.

In the analysis described above, the [^{88}SLRGG^{92},W^{110}/^{88}AAAAA^{92},A^{110}]scIL-5 asymmetric mutant affinity for the shIL-5Rα-Fc was lower than that for the single-chain IL-5 protein. A similar affinity relationship was observed in a second set of experiments using a sandwich assay protocol (*22*, *23*), in which the single-chain IL-5 and the [^{88}SLRGG^{92}, W^{110}/^{88}AAAAA^{92},A^{110}]scIL-5 asymmetric mutant were anchored to the 4A6 antibody and IL-5Rα-Fc was used as the analyte (data not shown).

The ability of [^{88}SLRGG^{92},W^{110}/^{88}AAAAA^{92},A^{110}]scIL-5 mutant to induce signal was measured by TF-1 cell proliferation. The proliferation curves for the single-chain mutant and normal sequence control are shown in Figure 5A. The asymmetric mutant containing the CD loop mimotope ^{88}SLRGG^{92} and the E110W mutation exhibited an abruptly reduced bioactivity, with an EC_{50} value of 4.78 nM compared to an EC_{50} of 0.036 nM for the single-chain IL-5 (that is more than 2 orders of magnitude lower than the bioactivity for the mutant). This EC_{50} value obtained for the [^{88}SLRGG^{92}, W^{110}/^{88}AAAAA^{92},A^{110}]scIL-5 mutant strongly suggests that, when one-half of the single-chain IL-5 is disabled, ^{88}EE-RRR^{92} and Glu110 replacements in the other half with ^{88}SLRGG^{92} and Trp, respectively, result in a molecule with preferentially suppressed ability to activate the receptor. The overall results obtained for the [^{88}SLRGG^{92},W^{110}/^{88}AAAAA^{92},

Table 1: Binding Parameters and Biological Activities of *E. coli*-Expressed scIL-5, [^{88}SLRGG^{92}-E110W/A6]scIL-5[a]

	scIL-5 proteins bind directly to immobilized IL-5Rα-Fc			proliferation assays
variant[b]	k_{on} ($\times 10^5$ M^{-1} s^{-1})	k_{off} ($\times 10^{-3}$ s^{-1})	K_d (nM)	EC_{50} (pM)
scIL-5	6.3 ± 0.1	10.3 ± 0.9	16.3 ± 1.4	36.3 ± 0.9
[^{88}SLRGG^{92}/A5]scIL-5	5.0 ± 0.1	7.8 ± 0.4	15.6 ± 1.0	93.8 ± 12.7
[E110W/A6]scIL-5	0.2 ± 0.03	9.5 ± 2.1	475.0 ± 126.9	2835.3 ± 97.8
[^{88}SLRGG^{92}-E110W/A6]scIL-5	0.33 ± 0.06	10.2 ± 0.1	309.1 ± 16.7	4783.0 ± 103.5

[a] The table compares the results obtained here with those reported previously for E110W variants of scIL-5. [b] The binding parameters and bioactivity data for scIL-5 and [E110W/A6]scIL-5 are reported in ref *25*. The data for [^{88}SLRGG^{92}/A5]scIL-5 are reported in ref *23*.

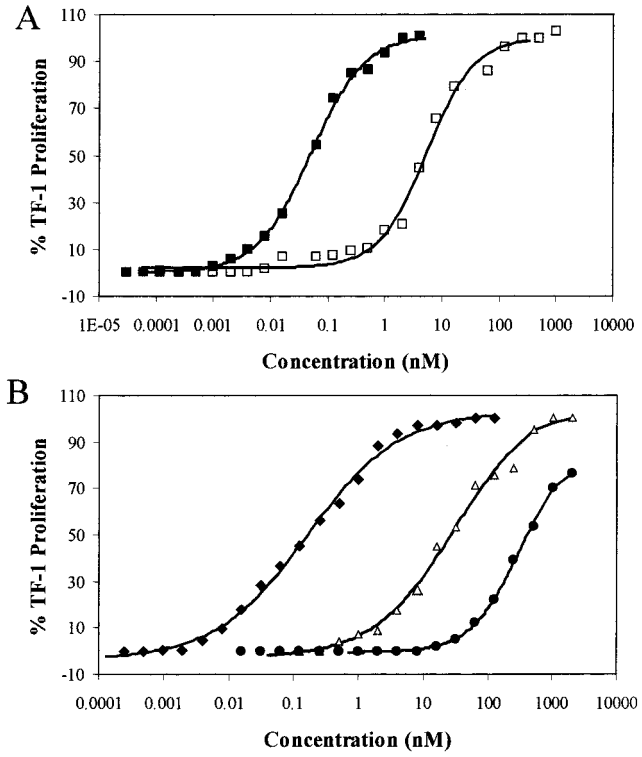

FIGURE 5: TF-1 proliferation of single-chain IL-5 and GM1 variants: (A) single-chain IL-5 (■) and [^{88}SLRGG^{92},W^{110}/^{88}AAAAA^{92},A^{110}]scIL-5 (□) and (B) GM1 (◆), [A^{13},A^{110}]GM1 (△), and [^{88}SLRGG^{92},W^{110}]GM1 (●). The EC_{50} values from these data are shown in Tables 1 and 2 and are the results of three separate experiments carried out in triplicate.

A^{110}]scIL-5 asymmetric mutant suggested the possibility of designing a smaller IL-5 mimetic antagonist lead by retaining an IL-5 receptor α-chain binding epitope in the region of residues 88−92 and suppressing activation by eliminating epitopes analogous to Glu110.

It should be noted that the EC_{50} value for unmutated scIL-5 is several orders of magnitude smaller than the K_d for receptor binding (see Table 1). This phenomenon has been observed before for wild-type IL-5 and for all IL-5 forms investigated to date, whether selectively mutated or not (*24*), and also is seen with the monomeric IL-5 analyses shown below. Its mechanistic basis is uncertain but could originate from the ability of cells to generate signals at partial receptor occupancy.

The data of Table 1 compare the results obtained here for [^{88}SLRGG^{92},W^{110}/^{88}AAAAA^{92},A^{110}]scIL-5 with results for other scIL-5 species obtained previously. The current scIL-5 mutant contains a combination of mutations of residues 88−92 and Glu110, while the previous mutants were modified in either one sequence region or the other. Importantly, combining mutations of residues 88−92 and E110 did not eliminate receptor binding and reinforced the notion that simultaneous mutations at these two sites could be used to help differentiate receptor recognition and receptor activation. This combination thus provided a basis for then moving on to the GM1 mutants to further establish the differentiability of epitopes for receptor activation and receptor recognition.

Receptor Binding Activities for the GM1 Monomers. We then turned to GM1 to further test the feasibility of designing lower-molecular mass IL-5 mutants with selectively suppressed bioactivity versus receptor affinity. We focused this study on two GM1 mutants, namely, [A^{13},A^{110}]GM1 and [^{88}SLRGG^{92},W^{110}]GM1. Both of these constructs retain a sequence in the region of residues 88−92 which we predicted would support receptor binding but which contain replacements for Glu110 and, in one case, a second activation-involved residue, Glu13. To determine the affinities of the GM1 monomers for the shIL-5Rα-Fc, the optical biosensor methodology was used. Typical sensorgram data are shown in Figure 6. In a first biosensor experiment, the shIL-5Rα-Fc was immobilized on the sensor chip and the GM1 monomers were used as analytes. Optimal experimental conditions were obtained by generating two surface densities, namely, 2000 and 7000 RU, and the flow rate was 30 μL/min. The association and dissociation rates, k_a and k_d, respectively, and the equilibrium dissociation constant, K_d, were calculated by globally fitting the association and dissociation phases of sensorgrams to a 1:1 Langmuir binding model. In the cases of direct binding data (Figure 6A,C), fits were to initial association and dissociation data to account for apparent instrument-derived artifacts at longer association times and at the buffer change interfaces. The rate constants k_a and k_d and the equilibrium dissociation constant K_d were calculated as an average of those determined for each surface density. The results for GM1 and GM1 mutants are summarized in Table 2.

The K_d values of *E. coli*-expressed GM1 monomers for the shIL-5Rα-Fc as determined in this methodology are 38.9, 585, and 69.4 nM for GM1, [A^{13},A^{110}]GM1, and [^{88}SLRGG^{92},W^{110}]GM1, respectively. It is worth stressing that the replacement of ^{88}EERRR^{92} with ^{88}SLRGG^{92} in the IL-5 monomeric construct GM1 and the Glu110 with Trp led to an affinity for the shIL-5Rα-Fc of this mutant that was only about 2-fold lower compared to that of the parent GM1. A more pronounced effect was obtained by disabling the binding epitope Glu110 with Ala, in the dual mutation of both Glu13 and Glu110 to Ala. In this case, the affinity for the receptor decreased about 15-fold. The association of [^{88}SLRGG^{92},W^{110}]GM1 is 4-fold slower than that of parent GM1, while the dissociation is about 2-fold slower. For the [A^{13},A^{110}]GM1 monomer versus parent GM1, the association rate is similar but the dissociation is much faster.

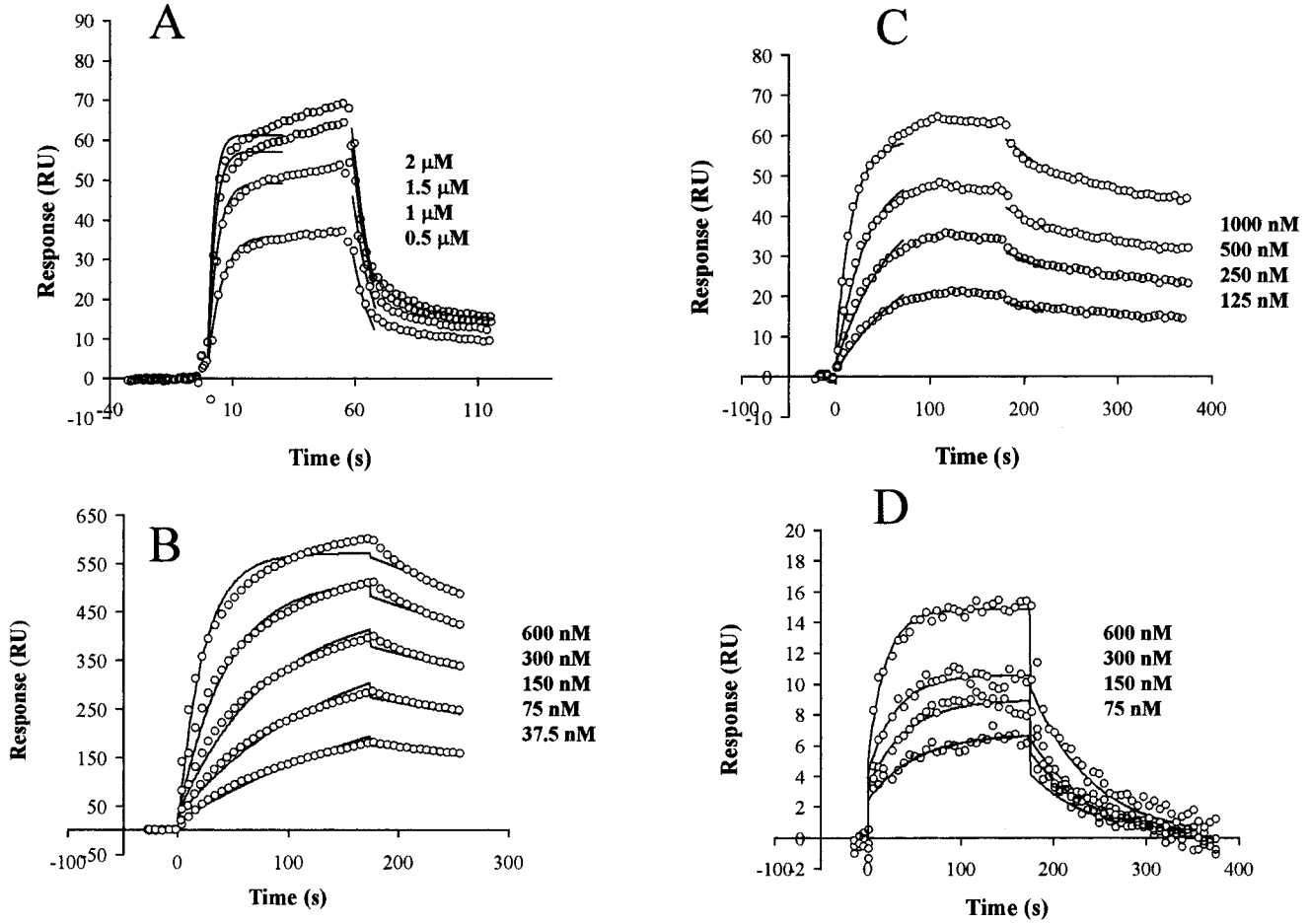

FIGURE 6: Sensorgram overlays for [A[13],A[110]]GM1 and [[88]SLRGG[92],W[110]]GM1 binding to shIL-5Rα-Fc at different analyte concentrations. The analyte concentrations are shown at the right of each sensorgram. (A and C) Sensorgrams for [A[13],A[110]]GM1 and [[88]SLRGG[92],W[110]]-GM1 as analytes binding directly to the immobilized shIL-5Rα-Fc on the sensor chip, at surface densities of 7000 and 2000 RU, respectively. (B and D) Binding of shIL-5Rα-Fc as an analyte to antibody-anchored [A[13],A[110]]GM1 and [[88]SLRGG[92],W[110]]GM1, with an antibody surface density of 3000 RU and a capture level of 250 RU. The rate constants for binding to shIL-5Rα-Fc were calculated by globally fitting the association and dissociation phases of the sensorgrams to a 1:1 Langmuir model (A + B ⇔ AB), as described in Experimental Procedures.

Table 2: Binding Parameters and Biological Activities of *E. coli*-Expressed Multisite Mutants of Single-Chain IL-5 and GM1[a]

	direct binding of single-chain IL-5 proteins to the immobilized IL-5Rα-Fc			binding of IL-5Rα-Fc to single-chain IL-5 proteins captured by 4A6 mAb			TF1 proliferation
variant	k_a ($\times 10^5$ M^{-1} s^{-1})	k_d ($\times 10^{-3}$ s^{-1})	K_d (nM)	k_a ($\times 10^5$ M^{-1} s^{-1})	k_d ($\times 10^{-3}$ s^{-1})	K_d (nM)	EC_{50} (nM)
GM1	1.94 ± 0.05	7.5 ± 0.3	38.6 ± 1.81	0.68 ± 0.08	1.05 ± 0.18	15.4 ± 3.2	0.164 ± 0.021
[A[110],A[13]]GM1	1.69 ± 0.05	98.8 ± 0.5	584.6 ± 17.5	0.7 ± 0.08	1.6 ± 0.06	22.8 ± 2.73	27 ± 2.3
[[88]SLRGG[92],W[110]]GM1	0.53 ± 0.1	3.68 ± 0.1	69.4 ± 13	0.66 ± 0.2	14.9 ± 0.17	225 ± 68	421.2 ± 27.4

[a] The rate constants k_a and k_d are from optical biosensor assays; the equilibrium constant K_d is calculated from the ratio of k_d/k_a. TF-1 cell proliferation activities are reported as the concentrations required for half-maximal stimulation from profiles as shown in Figure 5.

In another set of experiments, GM1 monomers were captured by the 4A6 antibody and shIL-5Rα-Fc was used as an analyte. The sensorgram data are shown in panels B and D of Figure 6 accompanied by the global fits to a 1:1 binding model. Other models were tested, including those for bivalent binding by analyte and conformational change, but these gave fits with greater deviation (greater χ^2 values). The K_d values obtained with the 1:1 model were 15.4 and 22.8 nM for GM1 and [A[13],A[110]]GM1, respectively, smaller than the K_d values determined in the direct binding assay. The finding of higher affinities of IL-5 constructs for the shIL-5Rα-Fc observed in the antibody-anchored configuration was also seen for [[88]SLRGG[92],W[110]/[88]AAAAA[92],A[110]]-scIL-5 above and has been previously reported for other single-chain IL-5 variants (*23*, *25*). One possible explanation for this is that capture of the ligand by the antibody prior to receptor binding could lead to stabilization of the ligand in a conformation that favors complexation. Another possibility is that the different methods of immobilization and molecules that were immobilized lead to different extents of exposure of binding sites of IL-5 mutants and receptor. In contrast, for the [[88]SLRGG[92],W[110]]GM1 variant, the equilibrium constant determined in the sandwich assay was 225 nM, greater than the equilibrium constant K_d determined in the direct binding assay. Hence, in this case, the antibody appears to negatively interfere with the stability or binding site access of the complex.

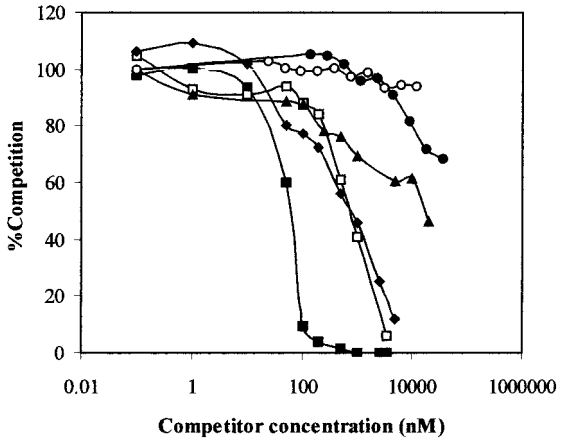

FIGURE 7: Competitive ELISA binding of single-chain IL-5 and GM1 mutants to shIL-5Rα. ELISA plates were coated with single-chain IL-5 and incubated overnight at 4 °C with a mixture of shIL-5Rα and different concentrations of (■) single-chain IL-5, (□) [^{88}SLRGG^{92},W^{110}/^{88}AAAAA^{92},A^{110}]scIL-5, (◆) GM1, (▲) [A^{13}, A^{110}]GM1, (●) [^{88}SLRGG^{92},W^{110}]GM1, and (○) GM-CSF. Detection of bound receptor was carried out as described in Experimental Procedures. The data that are shown are the means of three independent experiments carried out in triplicate.

Overall, the binding data for GM1 variants in Table 2 show that the affinity of the monomeric variants [A^{13},A^{110}]GM1 and [^{88}SLRGG^{92},W^{110}]GM1 for the shIL-5Rα-Fc are not dramatically changed versus GM1, especially in the direct binding assay.

Competition Assay of scIL-5 and GM1 Mutants in Binding to shIL-5Rα. The abilities of scIL-5 and GM1 monomer mutants to bind the shIL-5Rα were further tested in a competition ELISA. Single-chain IL-5 was coated on the microtiter plates, and then the plates were incubated with 100 μL of 50 nM shIL-5Rα (*31*) and different concentrations of scIL-5, GM1, or mutants, ranging from 0 to 40 μM, in PBS buffer overnight at 4 °C. As shown in Figure 7, scIL-5, GM1, and [^{88}SLRGG^{92},W^{110}/^{88}AAAAA^{92},A^{110}]scIL-5 were able to completely compete the binding of single-chain IL-5 to shIL-5Rα, while [A^{13},A^{110}]GM1 and [^{88}SLRGG^{92},W^{110}]-GM1 competed 40 and 60%, respectively, at the concentration range used in the assay.

Biological Activity of GM1 Mutants. Bioactivities were measured for the GM1 mutants by cell proliferation, with the data shown in Figure 5B. The insertion of the eight-amino acid loop, which enabled IL-5 to fold as the GM1 monomer, resulted in an *E. coli*-expressed protein that also elicits biological activity, with an EC_{50} of 0.164 nM, which is 5-fold greater than that of *E. coli*-expressed scIL-5 (Table 2 vs Table 1). The [A^{13},A^{110}]GM1 monomer, in which both Glu13 and Glu110 residues that have been shown to be important in the biological activity of IL-5 and hence receptor activation were mutated to Ala, showed more than 100-fold decreased biological activity compared to the GM1 monomer.

The most abruptly decreased biological activity was observed in the [^{88}SLRGG^{92},W^{110}]GM1 mutant, in which the CD loop ^{88}EERRR^{92} is replaced with SLRGG and Glu110 is replaced with Trp. The EC_{50} value determined for this monomer was 421.2 nM, reflecting a more than 10^4-fold reduced biological activity compared to that of GM1.

DISCUSSION

In this work, we have evaluated the mechanistic hypothesis that receptor binding and receptor activation epitopes in IL-5 are separable and the consequent potential to design molecules with increasingly receptor antagonist properties by retaining essential features of the former while modifying the latter. Through this mechanism-based strategy, we have been able to obtain IL-5 mutants with selectively suppressed proliferation activities versus receptor binding affinities by multisite mutagenesis of both single-chain dimeric IL-5 and monomeric GM1. The central focus of our mutations was Glu110 combined with the receptor recognition sequence of residues 88−92. We recently obtained evidence that Glu110 plays an important role in receptor activation (*25*). We first tested the approach of Glu110-based multisite mutagenesis using an asymmetrically disabled scIL-5 in which one of the helix bundle domains was functionally disabled by six Ala replacements at residues 88−92 and 110, while the second half contained the CD loop mimotope ^{88}SLRGG^{92} and the E110W mutation. The comparative receptor recognition versus bioactivity properties (Table 1) of the resulting mutant [^{88}SLRGG^{92},W^{110}/^{88}AAAAA^{92},A^{110}]scIL-5 argue that ^{88}SLRGG^{92} and W^{110} can bind the IL-5 receptor α-chain with suppressed activation of the β_c-chain and hence encouraged us to introduce multisite mutations into the IL-5 monomer GM1. Dual replacement in a GM1 background of both the CD loop ^{88}EERRR^{92} and E110 with SLRGG and Trp, respectively, led to a monomeric protein, similar to the nondisabled half of the scIL-5 mutein, which retained a high affinity for the IL-5 receptor α-chain but exhibited suppressed bioactivity as determined by the extremely low ability to stimulate TF-1 cell proliferation. Furthermore, the combined mutation of Glu110 and Glu13 to Ala in GM1 led to a protein designated [A^{13},A^{110}]GM1 with selectively suppressed bioactivity. The greater quantitative effects of mutation on bioactivity than on receptor affinity for the above scIL-5 and GM1 multisite muteins are evident from the comparison of the data shown in Figure 8.

A key starting point for this work was the finding (*25*), by sequence randomization analysis of the Glu110 binding epitope, that IL-5 variant molecules with replacement of residue 110 with a nonpolar but hydrogen bond-facilitating Trp retain significant affinity for the IL-5 receptor α-chain. This result was surprising given the developing view (*24*) that Glu89, Arg91, and Glu110 form a triad of charged residues making up the pharmacophore for IL-5 receptor α-chain binding. Nonetheless, the mutant designated [E110W/^{88}AAAAA^{92},A^{110}]scIL-5 (*25*), when expressed and purified from *E. coli*, had a high affinity for the IL-5 receptor α-chain. Strikingly, though, this mutant exhibited a suppressed bioactivity, as determined by its ability to stimulate TF-1 cell proliferation. This observation led to the hypothesis that the side chain (likely the negative charge) of the E110 residue plays an important role in receptor activation and that, in the [E110W/^{88}AAAAA^{92},A^{110}]scIL-5 mutant (*25*), the IL-5 receptor α-chain could be recruited but into a nonactivating orientation. Hence, we suspected that mutation of Glu110 could lead to IL-5 mimetics with improving antagonist properties. The bioactivity-suppressed properties of both monomeric and single-chain IL-5 mutants made in the current

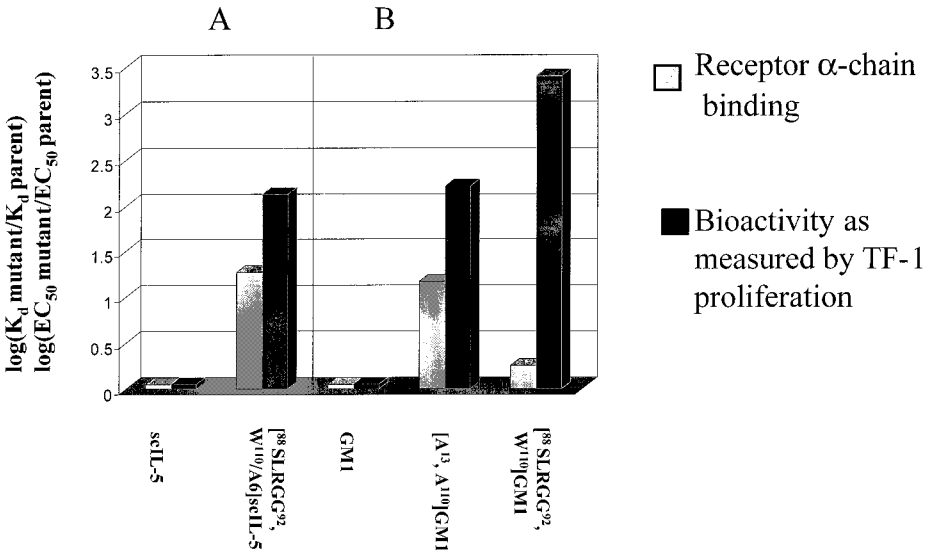

FIGURE 8: Bar graph of the disproportionate suppression of bioactivity vs receptor binding affinity observed with single-chain and monomeric IL-5 multisite mutants. The relative index of inactivation is given as log[activity of protein/activity of reference], where the reference is either scIL-5 (A) or GM1 (B). The index for the IL-5 receptor α-chain K_d is given in gray bars and for the TF-1 proliferation EC_{50} in black bars.

study confirm the importance of Glu110 in receptor activation.

The view that Glu110 mutations can allow the design of increasingly antagonistic IL-5 mutants must be considered in light of the previous and well-established finding that Glu13 also is a key component of receptor activation. Variants of wild-type and single-chain IL-5 in which the Glu13 residue was replaced with Ala retain the ability to specifically bind the α-chain (*19*, *20*) but exhibited reduced bioactivity. Similar behavior has been observed also in the other two cytokines sharing the β_c-chain, namely, IL-3 and GM-CSF. Here also, an important β_c-chain activation residue is located on the first helix, Glu21 for GM-CSF (*34*) and Glu22 for IL-3 (*35*). For IL-5 monomers, charge reversal of Glu13 in two circularly permutated monomeric constructs, designated IL-5.cT29 and IL-5.cT63, was reported by Edgerton et al. (*16*). In the case of the permutated monomer IL-5.cT29 with the Glu13Lys mutation**,** this variant exhibited only a modest reduction in the extent of TF-1 proliferation versus the Glu13 form of this monomer. In general, Glu13 mutations in IL-5 and its re-engineered forms lead to partial antagonists. This has led to the view that other residues besides Glu13 must participate in receptor activation (*24*). Glu110 appears to be such an additional residue. Indeed, the results obtained here with the [A^{13},A^{110}]GM1 monomer confirm that dual mutation of Glu13 and Glu110 can lead to greater selective suppression of IL-5 bioactivity. Thus, the monomeric variant [A^{13},A^{110}]GM1 exhibited a decrease in the extent of TF1 cell proliferation of more than 2 orders of magnitude compared to that of the *E. coli*-expressed GM1 (Figure 8) and 10^4-fold lower than that of wild-type IL-5 (*30*), while still retaining a significant affinity for the IL-5 receptor α-chain (K_d of 585 nM in the direct binding assay).

The overall results of this work argue for the feasibility to design smaller IL-5 receptor antagonists for therapeutic use in asthma and other eosinophilia-associated disease. Previous results with Glu110 randomization (*25*) and the current work argue that IL-5 possesses separable epitopes for α-chain binding (in particular, the region of residues 88−92) and receptor activation (including Glu13 and Glu110). Both the wild-type sequence ^{88}EERRR^{92} and the mimotope sequence ^{88}SLRGG^{92} are able to support receptor α-chain recruitment. However, without Glu13 and Glu110, this α-chain recruitment will be substantially nonactivating. Hence, smaller molecules retaining the wild-type charge balance in residues 88−92 may be able to bind sufficiently to the IL-5 receptor α-chain to function as antagonists.

ACKNOWLEDGMENT

We thank Dr. Jonas Johansson and Dr. K. S. Reddy (Department of Biochemistry and Biophysics, University of Pennsylvania) for the use of their Aviv spectropolarimeter and for their assistance with circular dichroism measurements. We are grateful to Dr. Gabriela Canziani for help and discussion concerning optical biosensor experiments.

REFERENCES

1. Karlen, S., De Boer, M. L., Lipscombe, R. J., Lutz, W., Mordvinov, V. A., and Sanderson, C. J. (1989) *Int. Rev. Immunol. 16*, 227−247.
2. Sanderson, C. (1998) in *IL-5: From Molecule to Drug Target for Asthma* (Sanderson, C., Ed.) Marcel Dekker, New York.
3. Egan, R. W., Chou, C.-C., Chapman, R. W., Jenh, C.-H., and Kung, T. T. (1999) in *IL5: From Molecule to Drug Target for Asthma* (Sanderson, C., Ed.) pp 321−329, Marcel Dekker, New York.
4. Bazan, J. F. (1990) *Proc. Natl. Acad. Sci. U.S.A. 87*, 6934−6938.
5. Cosman, D. (1993) *Cytokine 5*, 95−106.
6. Nicola, N. A. (1995) *Ann. N.Y. Acad. Sci. 766*, 253−262.
7. Tavernier, J., Devos, R., Cornelis, S., Tuypens, T., Van der Heyden, J., Fiers, W., and Plaetinck, G. (1991) *Cell 66*, 1175−1184.
8. Lopez, A. F., Elliott, M. J., Woodcock, J., and Vadas, M. A. (1992) *Immunol. Today 13*, 495−500.
9. Murata, Y., Takaki, S., Migita, M., Kikuchi, Y., Tominaga, A., and Takatsu, K. (1992) *J. Exp. Med. 175*, 341−351.
10. Devos, R., Guisez, Y., Cornelis, S., Verhee, A., Van der Heyden, J., Manneberg, M., Lahm, H. W., Fiers, W., Tavernier, J., and Plaetinck, G. (1993) *J. Biol. Chem. 268*, 6581−6587.

11. Mita, S., Tominaga, A., Hitoshi, Y., Sakamoto, K., Honjo, T., Akagi, M., Kikuchi, Y., Yamaguchi, N., and Takatsu, K. (1989) *Proc. Natl. Acad. Sci. U.S.A. 86*, 2311−2315.
12. Bazan, J. (1990) *Immunol. Today 11*, 350−354.
13. Proudfoot, A. E., Fattah, D., Kawashima, E. H., Bernard, A., and Wingfield, P. T. (1990) *Biochem. J. 270*, 357−361.
14. Milburn, M. V., Hassell, A. M., Lambert, M. H., Jordan, S. R., Proudfoot, A. E., Graber, P., and Wells, T. N. (1993) *Nature 363*, 172−176.
15. Li, J., Cook, R., Doyle, M. L., Hensley, P., McNulty, D. E., and Chaiken, I. (1997) *Proc. Natl. Acad. Sci. U.S.A. 94*, 6694−6699.
16. Edgerton, M. D., Graber, P., Willard, D., Consler, T., McKinnon, M., Uings, I., Arod, C. Y., Borlat, F., Fish, R., Peitsch, M. C., Wells, T. N., and Proudfoot, A. E. (1997) *J. Biol. Chem. 272*, 20611−20618.
17. Dickason, R. R., and Huston, D. P. (1996) *Nature 379*, 652−655.
18. Dickason, R. R., English, J. D., and Huston, D. P. (1996) *J. Mol. Med. 74*, 535−546.
19. Graber, P., Proudfoot, A. E., Talabot, F., Bernard, A., McKinnon, M., Banks, M., Fattah, D., Solari, R., Peitsch, M. C., and Wells, T. N. (1995) *J. Biol. Chem. 270*, 15762−15769.
20. Tavernier, J., Tuypens, T., Verhee, A., Plaetinck, G., Devos, R., Van der Heyden, J., Guisez, Y., and Oefner, C. (1995) *Proc. Natl. Acad. Sci. U.S.A. 92*, 5194−5198.
21. Cornelis, S., Plaetinck, G., Devos, R., Van der Heyden, J., Tavernier, J., Sanderson, C. J., Guisez, Y., and Fiers, W. (1995) *EMBO J. 14*, 3395−3402.
22. Morton, T., Li, J., Cook, R., and Chaiken, I. (1995) *Proc. Natl. Acad. Sci. U.S.A. 92*, 10879−10883.
23. Wu, S. J., Li, J., Tsui, P., Cook, R., Zhang, W., Hu, Y., Canziani, G., and Chaiken, I. (1999) *J. Biol. Chem. 274*, 20479−20488.
24. Chaiken, I. M., and Proudfoot, A. (1999) in *IL5: From Molecule to Drug Target for Asthma* (Sanderson, C., Ed.) pp 167−188, Marcel Dekker, New York.
25. Wu, S. J., Tambyraja, R., Zhang, W., Zahn, S., Godillot, A. P., and Chaiken, I. (2000) *J. Biol. Chem. 275*, 7351−7358.
26. Ames, R. S., Tornetta, M. A., McMillan, L. J., Kaiser, K. F., Holmes, S. D., Appelbaum, E., Cusimano, D. M., Theisen, T. W., Gross, M. S., Jones, C. S., et al. (1995) *J. Immunol. 154*, 6355−6364.
27. Laemmli, U. K. (1970) *Nature 227*, 680−685.
28. Monfardini, C., Ramamoorthy, M., Rosenbaum, H., Fang, Q., Godillot, P. A., Canziani, G., Chaiken, I. M., and Williams, W. V. (1998) *J. Biol. Chem. 273*, 7657−7667.
29. Jones, J. T., Ballinger, M. D., Pisacane, P. I., Lofgren, J. A., Fitzpatrick, V. D., Fairbrother, W. J., Wells, J. A., and Sliwkowski, M. X. (1998) *J. Biol. Chem. 273*, 11667−11674.
30. Li, J., Cook, R., Dede, K., and Chaiken, I. (1996) *J. Biol. Chem. 271*, 1817−1820.
31. Johanson, K., Appelbaum, E., Doyle, M., Hensley, P., Zhao, B., Abdel-Meguid, S. S., Young, P., Cook, R., Carr, S., Matico, R., et al. (1995) *J. Biol. Chem. 270*, 9459−9471.
32. Li, J., Cook, R., and Chaiken, I. (1996) *J. Biol. Chem. 271*, 31729−31734.
33. Myszka, D. G. (1999) *J. Mol. Recognit. 12*, 279−284.
34. Hercus, T. R., Bagley, C. J., Cambareri, B., Dottore, M., Woodcock, J. M., Vadas, M. A., Shannon, M. F., and Lopez, A. F. (1994) *Proc. Natl. Acad. Sci. U.S.A. 91*, 5838−5842.
35. Barry, S. C., Bagley, C. J., Phillips, J., Dottore, M., Cambareri, B., Moretti, P., D'Andrea, R., Goodall, G. J., Shannon, M. F., Vadas, M. A., et al. (1994) *J. Biol. Chem. 269*, 8488−8492.

BI001467P